Materials Sciences and Applications, 2023, 14, 208-221
https://www.scirp.org/journal/msa
ISSN Online: 2153-1188
ISSN Print: 2153-117X

# Optimize Multiple Peening Effects on Surface Integrity and Microhardness of Aluminum Alloy Induced by LSP

**Enoch Asuako Larson[1*], Samuel Adu-Gyamfi[2], Milku Augustine[3], Philip Yamba[4], Jamal-Deen Kukurah[4], Karimu Abdulai[5], Joseph Sekyi-Ansah[6], Osman Abdul-Razak[5], Emmanuel A. Akurugu[1], Aston Kuzmin[7]**

[1]School of Engineering, Department of Mechanical and Industrial Engineering, University for Development Studies, Tamale, Ghana
[2]Faculty of Engineering, Department of Mechanical Engineering, Sunyani Technical University, Sunyani, Ghana
[3]Faculty of Engineering, Department of Automobile Engineering, Bolgatanga Technical University, Bolgatanga, Ghana
[4]Faculty of Engineering, Department of Mechanical Engineering, Tamale Technical University, Tamale, Ghana
[5]School of Engineering, Department of Agricultural Engineering, University for Development Studies, Tamale, Ghana
[6]School of Engineering, Department of Mechanical Engineering, Takoradi Technical University, Takoradi, Ghana
[7]Department of Mechanization of Agricultural Products Processing, National Research Mordovia State University, Saransk, Russia
Email: *elarsonasuako@uds.edu.gh

**How to cite this paper:** Larson, E.A., Adu-Gyamfi, S., Augustine, M., Yamba, P., Kukurah, J.-D., Abdulai K., Sekyi-Ansah, J., Abdul-Razak, O., Akurugu, E.A. and Kuzmin, A. (2023) Optimize Multiple Peening Effects on Surface Integrity and Microhardness of Aluminum Alloy Induced by LSP. *Materials Sciences and Applications*, **14**, 208-221.
https://doi.org/10.4236/msa.2023.143012

**Received:** January 24, 2023
**Accepted:** March 20, 2023
**Published:** March 23, 2023



## Abstract

Laser shock peening is a modernized surface enhancement performed methodically to improve fatigue life, enhance the hardness of the material and make coarse grains flat under the superficial layer. In this current study, the effect of varying optimized multiple laser shock peening (LSP) is studied on the surface integrity, microhardness, and mechanical properties. The results show that the LSP-treated specimens have visible signs of valleys, wavy and varying height distribution as well as dimples. However, the presence of non-uniformity and sharp protrusions was detected from the superficiality of the as-received specimen and this was so because of the SiC abrasive material used to polish the superficial layer of the specimen before the test experiment. Prior to LSP, the surface roughness was 2 μm, however, after LSP the roughness increased to 4 μm, 6 μm and 17 μm for 1, 2, and 4 impacts, respectively. High-density dislocation can also be observed close to the grain boundary because the grain boundary prevents the migration of dislocation which could lead to dislocation walls and dislocation tangles. The increase in impacts decrease the average grain size, nevertheless, the micro-strain increased after multiple impacts. Furthermore, coarse grains after LSP were transformed into finer grains. The increase in the number of impacts increases the micro-strain likewise the full-width half maximum (FWHM). Finally, the in-

crease in microhardness increases as the LSP impacts increase.

## Keywords

Surface Integrity, Microhardness, Sharp Protrusions, SiC Abrasive Material, FWHM

## 1. Introduction

In the early 1960s, laser-induced shock waves were first studied and recognized [1]. Traditional shot peening (SP) was previously used in place of LSP, a more recent process of surface processing used to increase the fatigue life, wear, and corrosion resistance of metal materials [2] and control top surface crack initiation and propagation in thin sections [3] [4].

The under-study material aluminum alloy is incredibly useful in the automotive and aerospace industries due to its lightweight and average strength. However, its limitations in terms of material strength and corrosion resistance prevent its widespread use [4], and in recent years, techniques like LSP [5] [6], shot peening (SP), [7], surface attrition treatment [8], and ball burnishing [9] have drawn a lot of interest because it can enhance the mechanical properties of metal materials and in additive manufacturing as a post-treatment technique [10]. The influence of LSP on microstructure transformation and mechanical properties of metallic materials has been acknowledged by researchers [11] [12] [13] [14] and industry players.

Zhou *et al.* [14] examined the nano-crystallization of Ti-6AL-4V alloy produced via various LSP impacts. They [14] cited the existence of nano-crystalline in the metal alloy's top region. In addition, Zhou *et al.* [15] studied how repeated impacts affected the mechanical property and fatigue fracture morphology of 6061-T6 aluminum employed by laser shock peening (LSP). They established that as the LSP impacts increased, so did the state of residual compressive stress surface increased. In using a pulsed water jet peened on stainless steel surface, Srivastava M. *et al.* [16] investigated surface integrity and residual stress analysis. The outcome of the study revealed that due to the inhomogeneous plastic deformation generated by the pulsed water jet (PWJ) impact pressure and the water hammering effect, distinct sections of the surface were discovered to have irregularities and also a significant increase in the microhardness was observed with an initial hardness value from 347 HV to 570 HV.

Furthermore, Lu *et al.* [17] investigated how the mechanical characteristics and wear behaviors of AISI 8620 steel were affected by numerous LSP impacts with various pulse energies. The experiment results showed that as the number of LSP impacts increased, surface microhardness and roughness also increased. Finally, Multiple LSP on the mechanical properties and corrosion resistance of shipbuilding 5083Al alloy was investigated by Wang, H. *et al.* [18] in a simulative seawater environment. They indicated that after the multiple LSP impacts, the surface roughness alongside the microhardness of the material increased with a simultaneous increase in impacts.

Several studies have been performed on multiple LSP on metallic material. However, few researchers have focused on the effect of multiple impacts of LSP on surface integrity, mechanical property and microhardness on AA2024-T3 aluminum alloy. This has necessitated the need to optimize and perform an in-depth study on the effects of multiple peening on surface integrity, microhardness, and microstructure evolution. Varying the number of LSP impacts alters the surface integrity, microhardness and subsequently the effect it has on microstructure evolution in relation to optimum LSP parameters. The transmission electron microscope (TEM) was used to analyze the microstructure evolution. The microhardness and surface roughness were also investigated and analyzed chronologically by the hardness tester and the 3D surface roughness machine, respectively.

## 2. Experimental Methods

### 2.1. Specimen Preparation

The LSP experiment was performed on a square specimen with different peening impacts #1, #2 and #4 impacts, respectively. The square specimen size (width × length × thickness) 40 × 30 × 3 mm was wire cut and peened from a rolled sheet plate. The specimen was LSP treated with the same LSP parameters but different LSP impacts. The micro-strain and full-width half maximum (FWHM) were analyzed. Additionally, the specimen was also used to determine the microhardness and surface roughness. In all, a total of eight square specimens were used. Before LSP, the specimens were ground with SiC abrasive material with varying rough to fine grit grades, ranging from #140 to #2500 sequentially.

After, the specimen surface was polished using an ultrasonic polisher and then degreased in ethanol. To protect the surface material from the ablative effect of the LSP treatment, the treated area was covered with aluminum foil approximately 120 mm thick and a water-confining layer of about 2 mm thick. Figure 1 shows the square specimen used for the entire test.

### 2.2. Material Used

In this current study, the authors looked at a common material AA2024-T3 aluminum alloy; thus, the addition of alloy element to pure aluminum and tempering T3 to a process known as solution heat treatment, stress relieving at a controlled rate of stretching. The material is largely used in the aerospace industry for fastening devices, aircraft fittings and in the automotive space for automobile structures. The study material was selected as a result of its sterling strength-to-weight ratio, formability and corrosion resistance.

Table 1 and Table 2, represent both the chemical composition and mechanical properties of the material.

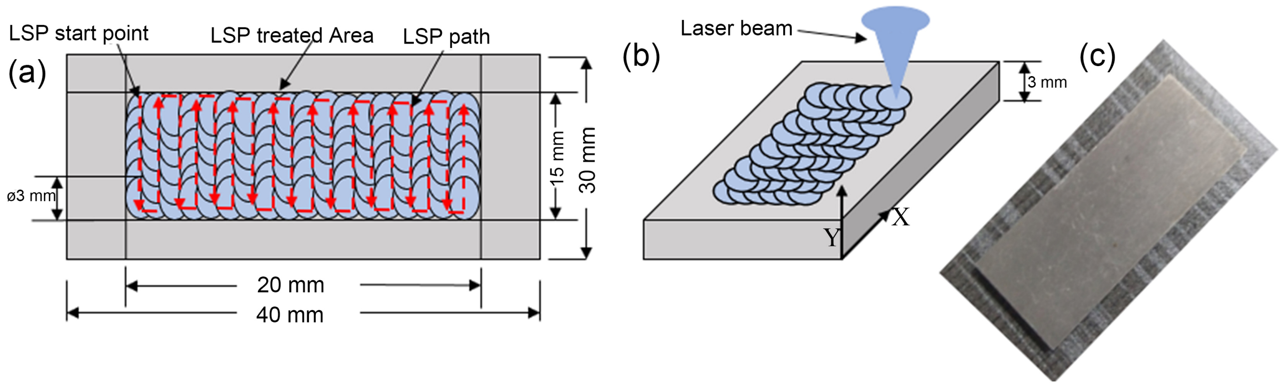


**Figure 1.** (a) Square specimen (b) 3D Square specimen with LSP zig-zag scanning pattern (c) AA 2024-T3 specimen.

**Table 1.** Chemical composition of Al2024-T3 aluminum alloy (wt%) [19].

| Cu | Mg | Mn | Si | Fe | Zn | Cr | Ti | Al |
|---|---|---|---|---|---|---|---|---|
| 5.3 | 2.07 | 0.67 | 0.01 | 0.08 | 0.04 | 0.09 | 0.05 | Bal. |

**Table 2.** Mechanical properties of Al 2024-T3 aluminum alloy [19].

| Tensile stress (MPa) | Yield stress (MPa) | Elongation (%) |
|---|---|---|
| 461 | 327 | 29.5 |

## 2.3. Experimental Setup

THALES laser, is high intensity Q-switched Nd:YAG (neodymium-doped yttrium aluminum garnet) with about ~8 - 10 ns pulse width, 1.064 μm wavelength, and a repetition rate of 5 Hz, was used for the LSP experiment. The output of the laser beam profile is a flat top with a ~25 mm beam size. The LSP processing was performed under atmospheric conditions. **Figure 2** shows the LSP experiment setup and **Table 3** shows the LSP processing parameters used. Prior to LSP, the parameters estimated were based on the following mathematical equations.

Laser induced pressure [20] [21];

$$P = 0.01\sqrt{\frac{\alpha}{2\alpha+3}}\sqrt{Z\left(\mathrm{g/cm^2m^1}\right)}\sqrt{I_o\left(\mathrm{GW/cm^2}\right)} \tag{1}$$

The peak density is expressed as in [22];

$$I_o = \frac{4E}{\pi d^2 \tau} \tag{2}$$

Reduced impedance [23] [24];

$$\frac{2}{Z} = \frac{1}{Z_1} + \frac{1}{Z_2} \tag{3}$$

Hugoniot Elastic Limit (HEL) [21];

$$\mathrm{HEL} = \frac{(1-v)\sigma_Y^{dyn}}{1-2v} \tag{4}$$

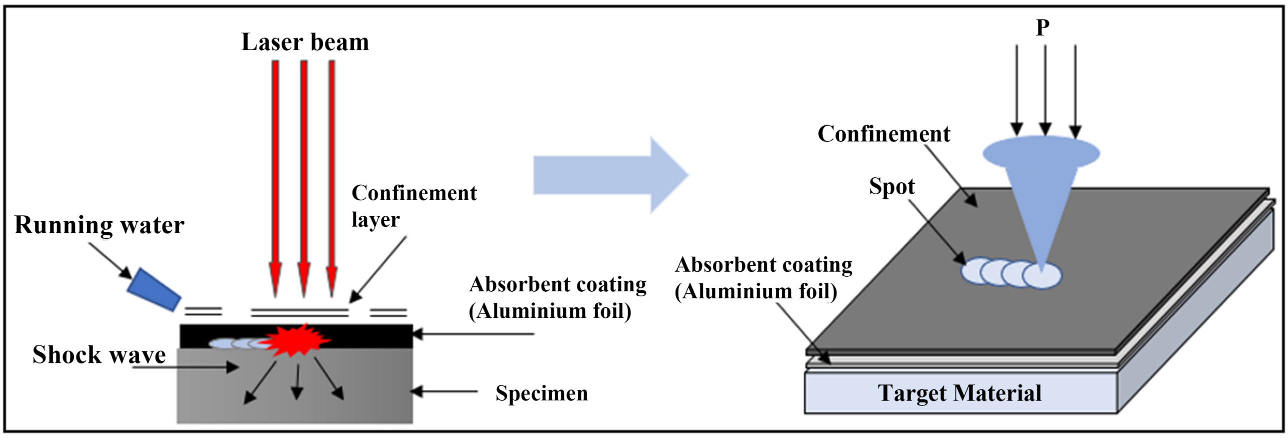


**Figure 2.** Illustration of LSP experiment.

**Table 3.** LSP Processing parameters of Al 2024-T3 aluminum alloy.

| Specimen | Number of LSP impacts | Overlapping ratio (%) | Laser Pulse Energy (J) | Spot diameter (mm) | Pulse width (ns) | Laser wavelength (μm) |
|---|---|---|---|---|---|---|
| $Specimen_0$ | 0 | 0 | 0 | 0 | 0 | 0 |
| $Specimen_1$ | 1 | 50 | 4 | 3 | 10 | 1.064 |
| $Specimen_2$ | 2 | 50 | 4 | 3 | 10 | 1.064 |
| $Specimen_3$ | 4 | 50 | 4 | 3 | 10 | 1.064 |

Now, $P$ denotes pressure induced via the shock wave (GPa), $Z$ stands for the reduced shock impedance, while $Z_1$ and $Z_2$ stand for the metallic material's shock impedance and the confining medium, respectively. $a$ is the size of the laser point in (cm$^2$), and $B$ is (21 or 10.1) depending on whether the medium is made of glass or water, respectively. $I_o$ represents the laser power density (GW/cm$^2$), $E$ denotes the laser pulse energy in (J), $d$ denotes the laser spot diameter in (cm), $\tau$ is the pulse duration in (ns), The Poisson ratio is defined by $v$, and the dynamic yield strength at high strain rates is denoted by $\left(\sigma_y^{dyn}\right)$.

## 2.4. Surface Roughness Measurement

Prior to laser treatment, both specimens the untreated and LSP treated were rough and fine polished ranging from 300 - 1500 μm grit with silicon carbon abrasive material in sequent, then finely polished with silk cloth and ethanol. The 3D laser microscope (KEYENCE, VK-250) model was made in Japan.

## 2.5. Microhardness Measurement

HXD-1000TMSC/LCD microhardness testing machine was employed to measure the surface of the material prior to and after laser shock peening. The specimens' surface was prepared as described in the surface roughness preparation section. The study was performed based on standard test ASTM standard E92-82. Ten different measurements were carried out and the average was recorded. 1.96 N load and time of 10 seconds were used.

### 2.6. XRD Diffraction (XRD) and Phase Analysis

The XRD analysis for both untreated and LSP treated specimens used the following parameters; Cu-K$\alpha$ radiation 40 kV, scan rate 5˚/min, step size 0.02, 30˚ ≤ 2$\theta$ ≤ 120˚ and 1.540598 Å radiation source and frequency, respectively. In the study, four lattice planes were fully considered which are $\alpha$-Al {111}, {200}, {220} and {311}. The full with half maximum (FWHM) of the Bragg diffraction peaks was calculated from the average grain size using William-Scherer [25] Equation,

$$FW \times \cos\theta = \frac{K\lambda}{D} + 4 \times \varepsilon \times \sin\theta \quad (5)$$

Now, from Equation (5) grain size denotes $D$, Scherer's factor of the lattice constant $K$, ($K$ = 0.9) when it is assumed to be in the shape of a sphere, lambda denotes wavelength for the X-ray, where $\lambda$ ($\lambda$ = 1.5418 Å), the micro-strain is denoted by $\varepsilon$, and finally, theta is the Bragg angle, $\theta$.

## 3. Results and Discussions

### 3.1. Surface Integrity Analysis

The surface integrity changes of AA2024-T3 aluminum alloy prior to, and after LSP treatment is compared and evaluated. Figure 3 represents the 3D surface contour roughness of the aluminum alloy prior to and after the LSP process with different processing impact. The impact of LSP and the subsequent effect on the

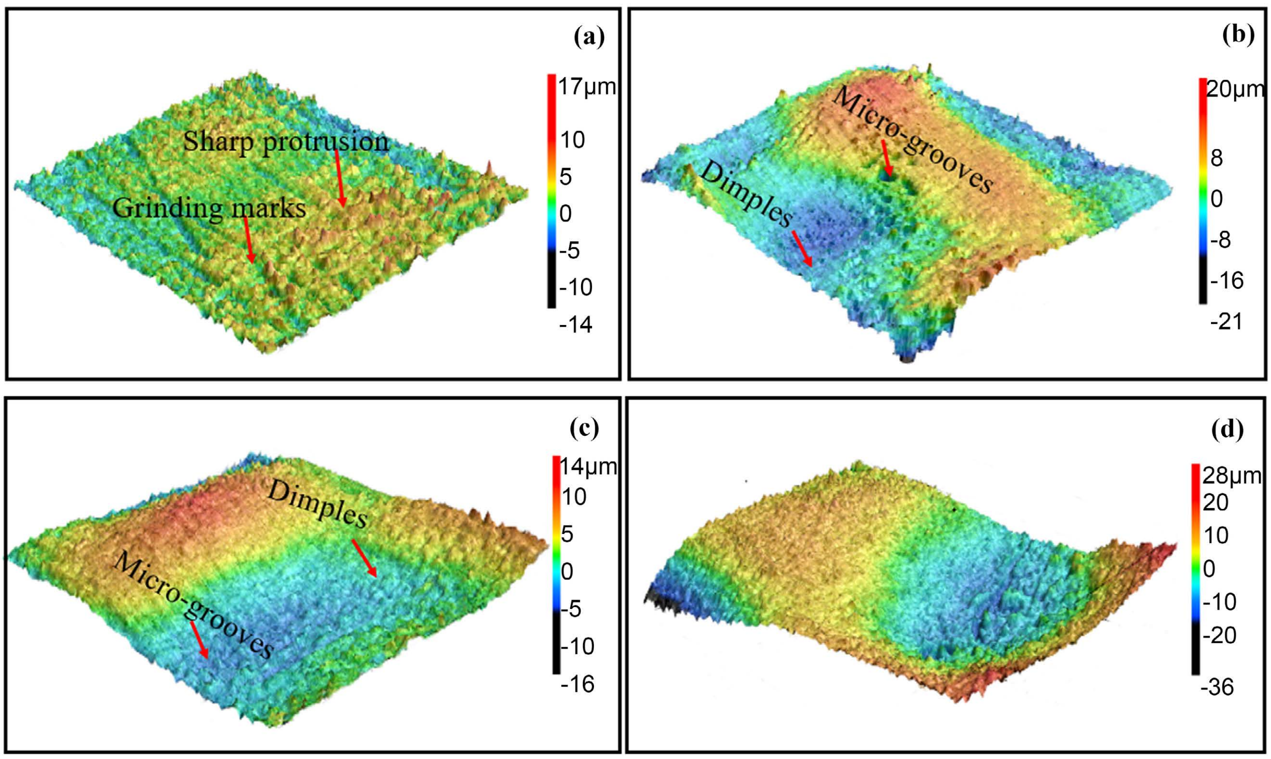


Figure 3. 3D surface contour roughness: (a) untreated, (b) 1 × LSP impact, (c) 2 × LSP impacts, and (d) 4 × LSP impacts.

specimen was used as a measure of surface flatness. The superficial layer of the LSP treated specimen profile shows enhance surface roughness because the specimen understudy is a soft material and the presence of plastic deformation induced after LSP is caused by the high pressure indentation from the shock-waves. The LSP treated specimens' shows visible signs of valleys, wavy and varying height distribution as well as dimples, this as a result of the increasing LSP impacts.

Furthermore, results from the material's plastic flow during LSP demonstrate that higher shock pressure levels exceed the material's Hugoniot Elastic Limit (HEL). Wang, H. *et al.* [18], Shu, S. *et al.* [26], and Maharjan, N. [27] published studies with comparable findings. In addition, the presence of non-uniform and sharp protrusions was observed from the top layer of the untreated material and this was obvious because of the SiC abrasive material used to polish the superficial layer of the specimen before the test experiment. After 1 impact, there was a decrease in the sharp protrusions, followed by further decrease after 2 and 4 impacts, indicating that LSP can reduce sharp protrusions. Shen *et al.* [28] reported of similar results. The reason for the suppression of wavy peaks to valleys is the use of laser shot indentation. It was observed that after 1 LSP impact, the specimen's top surface generated micro-grooves and dimples that resulted in the increment of the top surface roughness. The untreated specimen recorded a roughness (Ra) value of 2 μm but subsequently increased to 4 μm after 1 impact. However, the presence of plastic deformation produced by LSP is what caused the surface roughness to increase. The surface roughness increased to 6 μm, then afterward to 17 μm from 2 to 4 impacts, respectively.

Additional investigation of the profile by the confocal microscope is shown in **Figure 4**. A height profile of 179 μm for the untreated specimen was measured scattering between 12 μm - −12 μm. After 1 impact, the surface roughness scattering increased between 20 μm - and −20 μm. However, when the LSP was increased to 2 impacts the surface roughness scattering further increased between 34 μm - −34, and 40 μm - −40 μm for 2 and 4 impacts, respectively. This increment is the result of the multiple impacts on the aluminum alloy specimen. This study confirms the results of Luong *et al.* [29] who reported that the surface roughness of the understudy aluminum alloy 7075-T7651 material increased from the initial average of 0.444 to 0.519 μm after 3 LSP scans.

The surface roughness measurement shows that the LSP-treated specimens were significantly increased due to ablation and melting effect. Rozmus [30] stated that the surface roughness of Ti-6Al-4V alloy was increased between 0.1 to 0.82 μm after LSP.

**Figure 5(a)** shows the optical micrograph of the untreated specimen surface roughness whereas **Figures 5(b)-(d)** show the corresponding surface roughness effect after LSP. The surface demonstrates shallow depressions generated after LSP, which reveal that the material has undergone substantial plastic deformation.

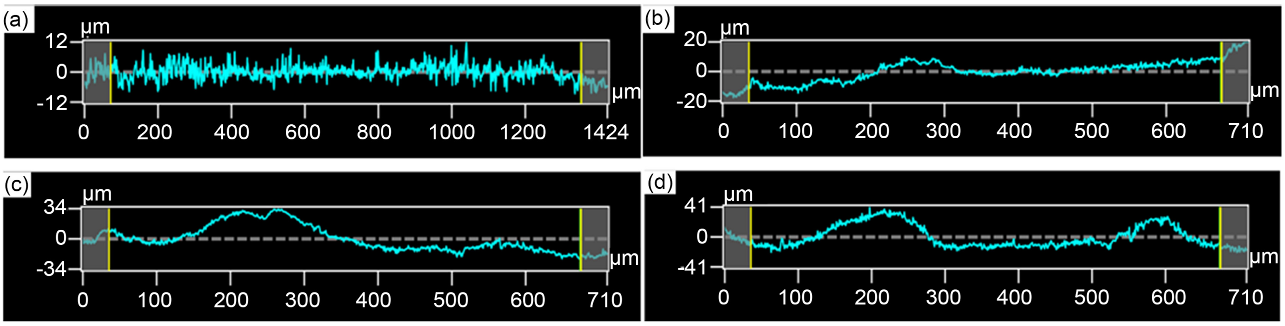


**Figure 4.** Surface cross-sectional profile: (a) untreated, (b) 1 × LSP impact, (c) 2 × LSP impacts, and (d) 4 × LSP impacts.

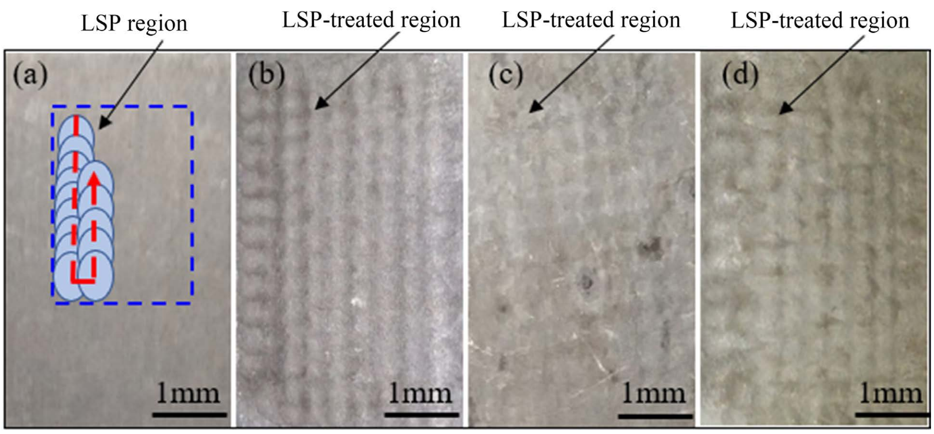


**Figure 5.** Optical micrograph of specimens prior to and after the LSP process. (a) Untreated (b) 1 × LSP impact (c) 2 × LSP impacts (d) 4 × LSP impacts on surface roughness.

### 3.2. TEM Observation

The TEM morphology was performed on the superficial layer at a depth between 0.1 to 0.2 μm as represented in Figures 6(a)-(c) showing dislocation cell, dislocation density, high-density dislocation line and grain boundary of the LSP-treated specimens. High-density dislocation could be observed close to the grain boundary because the grain boundary prevents the migration of dislocation which could lead to dislocation walls and tangles. From Figures 6(a)-(c), the 4 × LSP impacts were observed to have a greater dislocation density. This show that the superficial layer of AA2024-T3 aluminum alloy could experience substantial plastic deformation from LSP, which resulted in high-dislocation tangles and residual compressive stress in the interior grain. This principle explains the high strain rates induced by LSP treated specimens. Lu *et al.* [31] investigated how various LSP effects on the LY2 Al alloy affected the microstructure evolution and grain refinement mechanism. The changes of the DTs into sub-grain boundaries and the transformation of the dynamic recrystallization in sub-grain boundaries were to enhance the grain boundaries.

### 3.3. Effects of Multiple LSP Impacts on Mechanical Properties

#### 3.3.1. XRD Diffraction and Phase Analysis

Figure 7 shows the XRD pattern analysis for both untreated and LSP treated

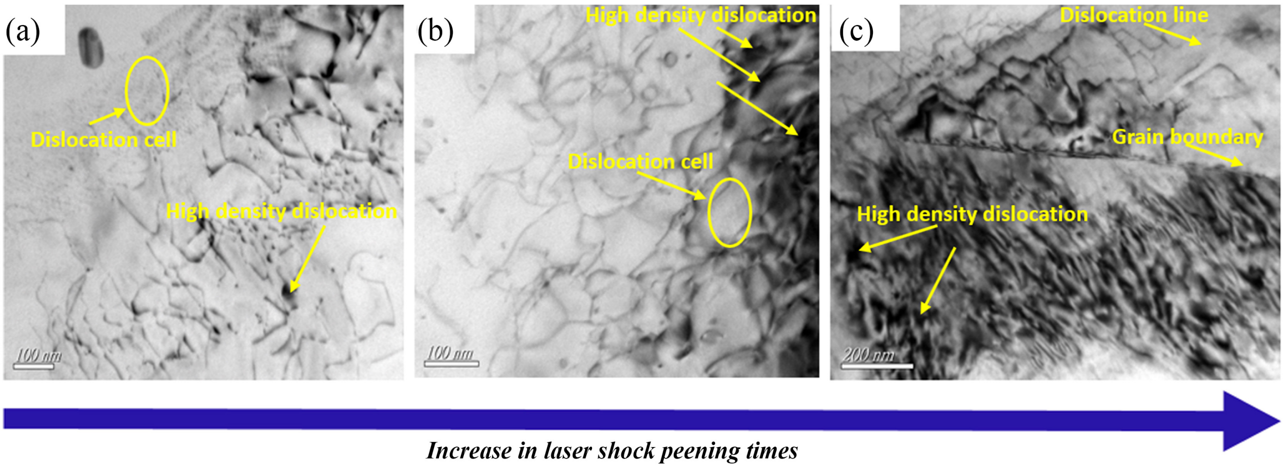


**Figure 6.** TEM bright field image. (a) 1 × LSP shot, (b) 2 × LSP shots, and (c) 4 × LSP shots.

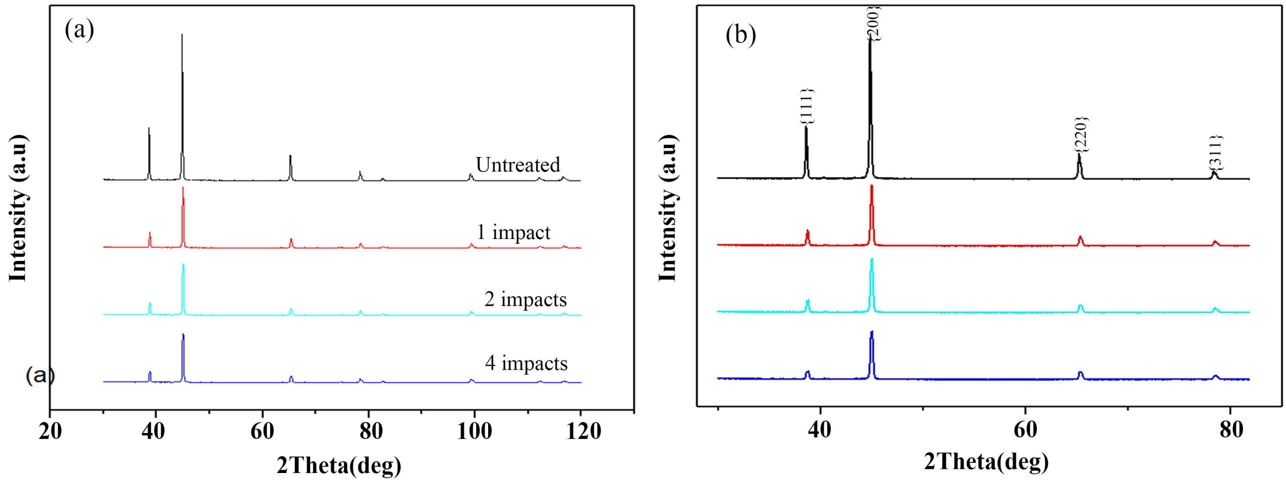


**Figure 7.** XRD pattern of the untreated and the LSP-treated specimens (a) Graph pattern (b) Magnified graph pattern.

materials. The results show that the width of FWHM peaks broadens as a result of multiple LSP impacts. The broadening effect was because of dislocation density resulting from micro- and high-strain plastic deformation in the peaks and crystal lattice [28] [30] and also grain refinement [22]. In addition, there were no additional diffraction peaks, crystalline phase and phase change observed after multiple LSP processes.

The increase in impact decreases the average grain size, nonetheless, the micro-strain increases after every multiple impact. Also, coarse grains after LSP were changed to finer grains which are attributed to the laser peening process.

Figure 8 shows the micro-strain and FWHM for AA2024-T3 aluminum alloy. The increase in multiple impacts increases the micro-strain likewise the FWHM. The peaks of the FWHM $\alpha$ (111), $\alpha$ (200), $\alpha$ (220) and $\alpha$ (311) for the untreated specimens were 0.1620, 0.1240, 0.1564 and 0.1456, respectively. However, after LSP 4 impacts the FWHM peaks $\alpha$ (111), $\alpha$ (200), $\alpha$ (220) and $\alpha$ (311) were enhanced to 0.298, 0.283, 0.284 and 0.350, respectively.

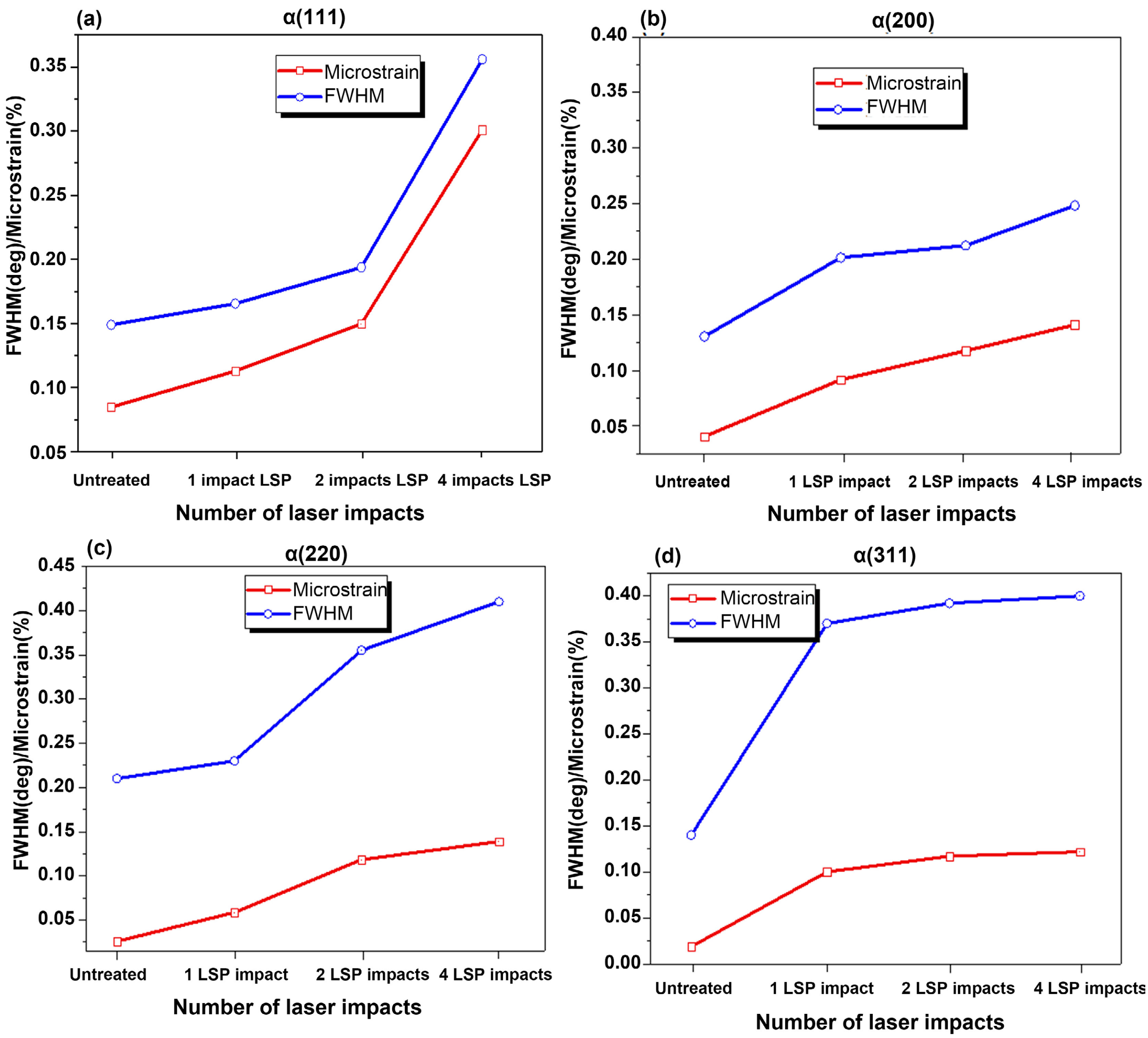


**Figure 8.** Micro-strain and FWHM of AA2024-T3 aluminum alloy.

#### 3.3.2. Microhardness Analysis

Figure 9 shows the microhardness of the untreated and LSP treated material measured along the length of the superficial layer. Results of the microhardness experiment revealed that the metallic material is resistant to indentation due to elastic plastic deformation [32] of the specimen. The microhardness for the untreated specimen understudy measured was 137 HV at normal room temperature. However, after 1 LSP impact, the hardness level was significantly enhanced to 168 HV, which shows an increment of 23% at the same prevailing room temperature. The increase to 2 LSP impact increased the hardness to 177 HV resulting in a 29% increment. Finally, the increase in the multiple impacts to 4 increases the hardness surface level to 190 HV, thus, resulting in a significant increase of 39%. This demonstrates that the hardness value increases as the number of LSP impacts increase resulting from grain size reduction or refinement,

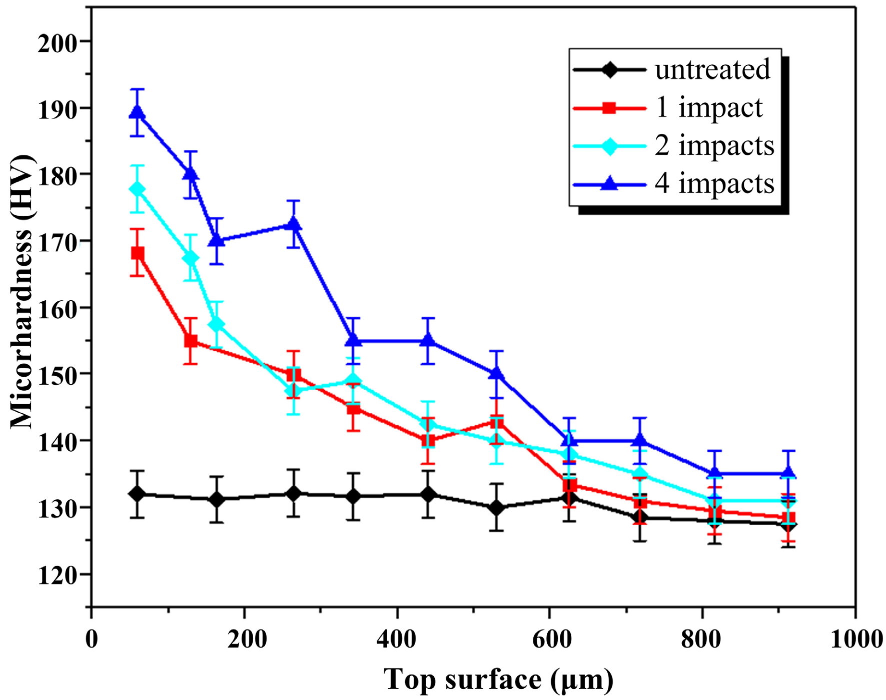


**Figure 9.** Microhardness surface profile on the cross-sectional view for untreated and LSP treated aluminum alloy.

dislocation density [33] [34] [35] and elastic plastic deformation [28] [32] on the surface of the material. Similar results are reported in the literature [16] [36]. Simge *et al.* [37] stated that the hardness for the untreated alloys for AA 6061-T6 via LSP was 97 HV. However, the highest hardness value for the LSP specimen was 118 HV. In their view, the impact from the high pressure laser irradiated the plastically deformed surface resulting in work hardening. Ren *et al.* [38] also stated that the hardness level impact by LSP was significantly enhanced in-depth with a gradual decrease.

## 4. Conclusions

The study looked at the effects of multiple LSP on surface integrity and microhardness of AA2024-T3 aluminum alloy. The study concludes on the:

Firstly, similar trends of the surface topography were exhibited just like the microhardness. The surface roughness increased as the number of times the LSP impact increased.

Secondly, there was no phase transformation after multiple laser shock peening impacts as observed from the XRD patterns. The broadening of the peaks meant grain refinement and dislocation multiplication as a result of the high strain rate and plastic deformation induced by LSP.

Finally, the microhardness value shows a good correlation that as the number of multiple impacts increased, both surface roughness and hardness increased with depth until they both reached their saturated limits.

Further research can be performed to investigate the fatigue life and other mechanical property on the surface enhancement.

## Acknowledgements

The authors are grateful to Prof. Dr. Xudong Ren (PhD supervisor), Professor Ren Yunpen, Dr. Wangfan Zhou and Dr. Tong all of Jiangsu University, P. R. China for the kind support during this research study.

## Conflicts of Interest

The authors declare no known conflict of interest.

## References

[1] Bantounas, I., Dye, D. and Lindley, T.C. (2010) The Role of Microtexture on the Faceted Fracture Morphology in Ti-6Al-4V Subjected to High-Cycle Fatigue. *Acta Materialia*, **58**, 3908-3918. https://doi.org/10.1016/j.actamat.2010.03.036

[2] Hatamleh, O., Lyons, J. and Forman, R. (2007) Laser and Shot Peening Effects on Fatigue Crack Growth in Friction Stir Welded 7075-T7351 Aluminum Alloy Joints. *International Journal of Fatigue*, **29**, 421-434. https://doi.org/10.1016/j.ijfatigue.2006.05.007

[3] Grum, J., Zupančič, M. and Ocaña, J.L. (2007) Laser Shock Processing of the Maraging Steel Surface. *Materials Science Forum*, **537**-**538**, 655-662. https://doi.org/10.4028/www.scientific.net/MSF.537-538.655

[4] Hong, Z. and Chengye, Y. (1998) Laser Shock Processing of 2024-T62 Aluminum Alloy. *Materials Science and Engineering*: *A*, **257**, 322-327. https://doi.org/10.1016/S0921-5093(98)00793-X

[5] Schijve, J. (2008) Fatigue of Structures and Materials. Springer, New York. https://doi.org/10.1007/978-1-4020-6808-9

[6] Prevéy, P.S., Jayaraman, N. and C.J., (2005) Overview of Low Plastcity Burnishing for Mitigation of Fatigue Damage Mechanisms. *Proceedings of ICSP* 9, Paris, 6-9 September 2005. http://citeseerx.ist.psu.edu/viewdoc/download?doi=10.1.1.505.2090&rep=rep1&type=pdf

[7] Cai, H. and McEvily, A.J. (2001) On Striations and Fatigue Crack Growth in 1018 Steel. *Materials Science and Engineering*: *A*, **314**, 86-89. https://doi.org/10.1016/S0921-5093(00)01925-0

[8] Fairand, B.P. and Clauer, A.H. (1979) Laser Generated Stress Waves: Their Characteristics and Their Effects to Materials. *Journal of Applied Physics*, **50**, 1497-1502. https://doi.org/10.1063/1.326137

[9] Jufang, C., Jiangtao, W., Xu, H.C. and Weining, L. (2011) Effect of Laser Surface Hardening on Pitting Corrosion Resistance of AM50 Magnesium Alloy. *International Conference on Advanced Technology of Design and Manufacture* (*ATDM* 2011), Changzhou, 3-5 November 2011, 1-4.

[10] Kalentics, N., de Seijas, M.O.V., Griffiths, S., Leinenbach, C. and Logé, R.E. (2020) 3D Laser Shock Peening—A New Method for Improving Fatigue Properties of Selective Laser Melted Parts. *Additive Manufacturing*, **33**, Article 101112. https://doi.org/10.1016/j.addma.2020.101112

[11] Wu, X., Huang, C., Wang, X. and Song, H. (2011) A New Effective Method to Estimate the Effect of Laser Shock Peening. *International Journal of Impact Engineer-*

*ing*, **38**, 322-329. https://doi.org/10.1016/j.ijimpeng.2010.11.008

[12] Dai, F., Lu, J.Z., Zhou, J.Z. and Luo, X. (2016) A Technique to Decrease Surface Roughness in Overlapping Laser Shock Processing. *Applied Surface Science*, **370**, 501-507. https://doi.org/10.1016/j.apsusc.2016.02.138

[13] Ren, X.D., *et al.* (2016) Dislocation Eution and Properties Enhancement of GH2036 by Laser Shock Processing: Dislocation Dynamics Simulation and Experiment. *Materials Science and Engineering*: *A*, **654**, 184-192. https://doi.org/10.1016/j.msea.2015.12.007

[14] Zhou, W., Ren, X., Liu, F., Ren, Y. and Li, L. (2016) Nanocrystallization in the Duplex Ti-6Al-4V Alloy Processed by Multiple Laser Shock Peening. *Metals*, **6**, Article 297. https://doi.org/10.3390/met6120297

[15] Zhou, J.Z., *et al.* (2012) Effect of Repeated Impacts on Mechanical Properties and Fatigue Fracture Morphologies of 6061-T6 Aluminum Subject to Laser Peening. *Materials Science and Engineering*: *A*, **539**, 360-368. https://doi.org/10.1016/j.msea.2012.01.125

[16] Srivastava, M., Hloch, S., Gubeljak, N., Milkovic, M., Chattopadhyaya, S. and Klich, J. (2019) Surface Integrity and Residual Stress Analysis of Pulsed Water Jet Peened Stainless Steel Surfaces. *Measurement*, **143**, 81-92. https://doi.org/10.1016/j.measurement.2019.04.082

[17] Lin, Y., Lu, J., Wang, L., Xu, T. and Xue, Q. (2006) Surface Nanocrystallization by Surface Mechanical Attrition Treatment and Its Effect on Structure and Properties of Plasma Nitrided AISI 321 Stainless Steel. *Acta Materialia*, **54**, 5599-5605. https://doi.org/10.1016/j.actamat.2006.08.014

[18] Wang, H., Huang, Y., Zhang, W. and Ostendorf, A. (2018) Investigation of Multiple Laser Shock Peening on the Mechanical Property and Corrosion Resistance of Shipbuilding 5083Al Alloy under a Simulated Seawater Environment. *Applied Optics*, **57**, 6300-6308. https://doi.org/10.1364/AO.57.006300

[19] Khodir, S.A. and Shibayanagi, T. (2007) Microstructure and Mechanical Properties of Friction Stir Welded Dissimilar Aluminum Joints of AA2024-T3 and AA7075-T6. *Materials Transactions*, **48**, 1928-1937. https://doi.org/10.2320/matertrans.MRA2007042

[20] Liao, Y., Suslov, S., Ye, C. and Cheng, G.J. (2012) The Mechanisms of Thermal Engineered Laser Shock Peening for Enhanced Fatigue Performance. *Acta Materialia*, **60**, 4997-5009. https://doi.org/10.1016/j.actamat.2012.06.024

[21] Cheng, G.J., Pirzada, D. and Ming, Z. (2007) Microstructure and Mechanical Property Characterizations of Metal Foil after Microscale Laser Dynamic Forming. *Journal of Applied Physics*, **101**, Article 063108. https://doi.org/10.1063/1.2710334

[22] Abeens, M., Muruganandhan, R., Thirumavalavan, K. and Kalainathan, S. (2019) Surface Modification of AA7075 T651 by Laser Shock Peening to Improve the Wear Characteristics. *Materials Research Express*, **6**, Article 066519. https://doi.org/10.1088/2053-1591/ab0b0e

[23] Bugayev, A.A., Gupta, M.C. and Payne, R. (2006) Laser Processing of Inconel 600 and Surface Structure. *Optics and Lasers in Engineering*, **44**, 102-111. https://doi.org/10.1016/j.optlaseng.2005.04.014

[24] Hill, M.R., Dewald, A.T., Rankin, J.E. and Lee, M.J. (2005) Measurement of Laser Peening Residual Stresses. *Materials Science and Technology*, **21**, 3-9. https://doi.org/10.1179/174328405X14083

[25] Williamson, G.K. and Hall, W.H. (1953) X-Ray Line Broadening from Filed Alumi-

nium and Wolfram. *Acta Metallurgica*, **1**, 22-31.
https://doi.org/10.1016/0001-6160(53)90006-6

[26] Shu, S., Huang, X., Cheng, Z., Shen, Y., He, Z. and Liu, W. (2021) Understanding the Relations between Surface Stress State and Microstructure Feature for Enhancing the Fatigue Performance of TC6 Titanium Alloy. *Coatings*, **11**, Article 1261.
https://doi.org/10.3390/coatings11101261

[27] Maharjan, N., Chan, S.Y., Ramesh, T., Nai, P.G. and Ardi, D.T. (2021) Fatigue Performance of Laser Shock Peened Ti6Al4V and Al6061-T6 Alloys. *Fatigue & Fracture of Engineering Materials & Structures*, **44**, 733-747.
https://doi.org/10.1111/ffe.13390

[28] Shen, X.j., Shukla, P., Nath, S. and Lawrence, J. (2017) Improvement in Mechanical Properties of Titanium Alloy (Ti-6Al-7Nb) Subject to Multiple Laser Shock Peening. *Surface and Coatings Technology*, **327**, 101-109.
https://doi.org/10.1016/j.surfcoat.2017.08.009

[29] Luong, H. and Hill, M.R. (2008) The Effects of Laser Peening on High-Cycle Fatigue in 7085-T7651 Aluminum Alloy. *Materials Science and Engineering: A*, **477**, 208-216.
https://doi.org/10.1016/j.msea.2007.05.024

[30] Rozmus-Górnikowska, M. (2018) Surface Modifications of a Ti6Al4V Alloy by a Laser Shock Processing. *Materials Research Society of Serbia*, **117**, 808-811.
http://przyrbwn.icm.edu.pl/APP/PDF/117/a117z519.pdf

[31] Lu, J.Z., *et al.* (2010) Grain Refinement of LY2 Aluminum Alloy Induced by Ultra-High Plastic Strain during Multiple Laser Shock Processing Impacts. *Acta Materialia*, **58**, 3984-3994. https://doi.org/10.1016/j.actamat.2010.03.026

[32] Fu, J., Zhu, Y., Zheng, C., Liu, R. and Ji, Z. (2015) Evaluate the Effect of Laser Shock Peening on Plasticity of Zr-Based Bulk Metallic Glass. *Optics & Laser Technology*, **73**, 94-100. https://doi.org/10.1016/j.optlastec.2015.04.009

[33] Cao, Z.W., Xu, H.Y., Zou, S.K. and Che, Z.G. (2012) Investigation of Surface Integrity on TC17 Titanium Alloy Treated by Square-Spot Laser Shock Peening. *Chinese Journal of Aeronautics*, **25**, 650-656.
https://doi.org/10.1016/S1000-9361(11)60429-9

[34] Guo, Y.B. and Caslaru, R. (2011) Fabrication and Characterization of Micro Dent Arrays Produced by Laser Shock Peening on Titanium Ti-6Al-4V Surfaces. *Journal of Materials Processing Technology*, **211**, 729-736.
https://doi.org/10.1016/j.jmatprotec.2010.12.007

[35] Jia, W., Hong, Q., Zhao, H., Li, L. and Han, D. (2014) Effect of Laser Shock Peening on the Mechanical Properties of a Near-$\alpha$ Titanium Alloy. *Materials Science and Engineering: A*, **606**, 354-359. https://doi.org/10.1016/j.msea.2014.03.108

[36] Clauer, A.H., Fairand, B.P. and Holbrook, J.H. (1981) Effects of Laser Induced Shock Waves on Metals. In: Meyers, M.A. and Murr, L.E., Eds., *Shock Waves and High-Strain-Rate Phenomena in Metals*, SpringerLink, Berlin, 675-702.
https://doi.org/10.1007/978-1-4613-3219-0_38

[37] Irizalp, S.G., Saklakoglu, N. and Yilbas, B.S. (2014) Characterization of Microplastic Deformation Produced in 6061-T6 by Using Laser Shock Processing. *The International Journal of Advanced Manufacturing Technology*, **71**, 109-115.
https://doi.org/10.1007/s00170-013-5481-0

[38] Ren, X.D., *et al.* (2013) Dislocation Polymorphism Transformation of 6061-T651 Aluminum Alloy Processed by Laser Shock Processing: Effect of Tempering at the Elevated Temperatures. *Materials Science and Engineering: A*, **578**, 96-102.
https://doi.org/10.1016/j.msea.2013.04.034